

Elliptic and triangular flow of light nuclei in Au+Au collisions in the BES-II energies using the STAR detector

Rishabh Sharma^{1,*}, for the STAR Collaboration

¹Indian Institute of Science Education and Research (IISER), Tirupati 517507, India

Abstract. Light nuclei might be formed in heavy-ion collisions by the coalescence of produced (anti-)nucleons or transported nucleons. Due to their low binding energies, they are more likely to form at later stages of the hadronic fireball. In this proceedings, we report the transverse momentum and centrality dependence of elliptic (v_2) and triangular (v_3) flow of d , t , and ${}^3\text{He}$ in Au+Au collisions at $\sqrt{s_{NN}} = 14.6 - 54.4$ GeV. The mass number scaling of $v_2(p_T)$ and $v_3(p_T)$ of light nuclei is discussed. We also report the comparison of $v_2(p_T)$ and $v_3(p_T)$ of light nuclei with a transport-plus-coalescence model calculation.

1 Introduction

High-energy heavy-ion collisions produce light nuclei in abundance. Thermal model proposes their formation near the chemical freezeout surface (CFO), however, due to their low binding energies it is unlikely that they survive at high CFO temperature [1]. In contrast, the coalescence model suggests their formation at later stages via nucleon recombination [2–5]. In the case of nucleon coalescence, the momentum space distributions of both the constituents (nucleons) and the products (light nuclei) are measurable in heavy-ion collision experiments. Therefore, studying the azimuthal anisotropy of light nuclei and comparing them with that of proton can give insights into the light nuclei production mechanism in heavy-ion collisions.

In the following sections, elliptic (v_2) and triangular (v_3) flow of d , t , and ${}^3\text{He}$ in Au+Au collisions at $\sqrt{s_{NN}} = 14.6, 19.6, 27, \text{ and } 54.4$ GeV are discussed.

2 Analysis details

The data presented in this proceedings are from Au+Au collisions at $\sqrt{s_{NN}} = 14.6, 19.6, 27, \text{ and } 54.4$ GeV collected by the STAR experiment at RHIC during the second phase of the Beam Energy Scan (BES-II) program. Light nuclei are identified using the Time Projection Chamber (TPC) [6] and the Time of Flight (TOF) [7] detectors. TPC uses specific ionization energy loss (dE/dx) in a large gas volume for nuclei identification. Further, the purity of light nuclei signal is enhanced by imposing a constraint on their mass-square (m^2), measured using the Time of Flight (TOF) detector.

The quantities v_2 and v_3 are the second and third order Fourier coefficients, respectively, characterizing the azimuthal distribution of the produced nuclei relative to the symmetry planes (called event planes) of the Au+Au collision. We have constructed the second (Ψ_2) and third (Ψ_3) order event plane angle using tracks reconstructed in the TPC. The η -subevent plane method is used to avoid auto-correlation [8].

*e-mail: rishabhsharma@students.iisertirupati.ac.in

3 Results

3.1 $v_2(p_T)$ and $v_3(p_T)$ of light nuclei

Figure 1 shows v_2 and v_3 of p , d , t , and ${}^3\text{He}$ as a function of p_T in 0-80% centrality interval in Au+Au collisions at $\sqrt{s_{NN}} = 14.6, 19.6, 27,$ and 54.4 GeV. In the measured p_T range, a monotonous increase in v_2 and v_3 of light nuclei with p_T is observed for all center-of-mass energies. Mass ordering of v_2 and v_3 is also observed at low p_T .

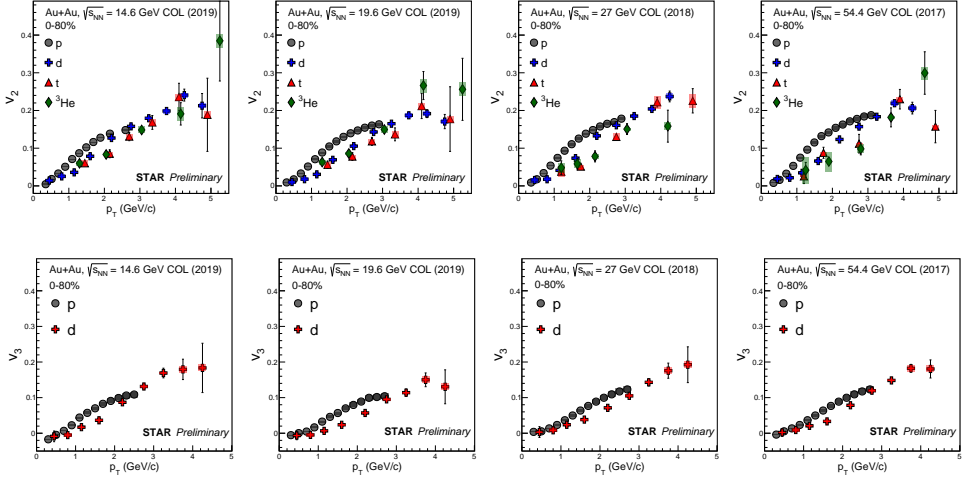


Figure 1. $v_2(p_T)$ (top panel) and $v_3(p_T)$ (bottom panel) of p , d , t , and ${}^3\text{He}$ in minimum bias Au+Au collisions at $\sqrt{s_{NN}} = 14.6, 19.6, 27,$ and 54.4 GeV. Vertical lines and shaded area at each marker represent statistical and systematic uncertainties, respectively.

3.2 Centrality dependence of $v_2(p_T)$ of light nuclei

Figure 2 shows the centrality dependence of $v_2(p_T)$ of d in Au+Au collisions at $\sqrt{s_{NN}} = 14.6, 19.6, 27,$ and 54.4 GeV. $v_2(p_T)$ of d is measured in 0-30% and 30-80% centrality ranges in Au+Au collisions. A clear centrality dependence of $v_2(p_T)$ is observed where peripheral collisions have higher v_2 values compared to central collisions. This observation can be explained by the fact that peripheral collisions have higher initial spatial anisotropy compared to central collisions, resulting in a higher v_2 value.

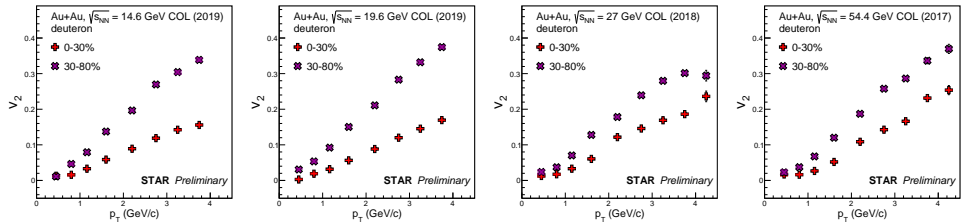


Figure 2. $v_2(p_T)$ of d measured in 0-30% and 30-80% centrality intervals in Au+Au collisions at $\sqrt{s_{NN}} = 14.6, 19.6, 27,$ and 54.4 GeV. Vertical lines and shaded bands at each marker represent statistical and systematic uncertainties, respectively.

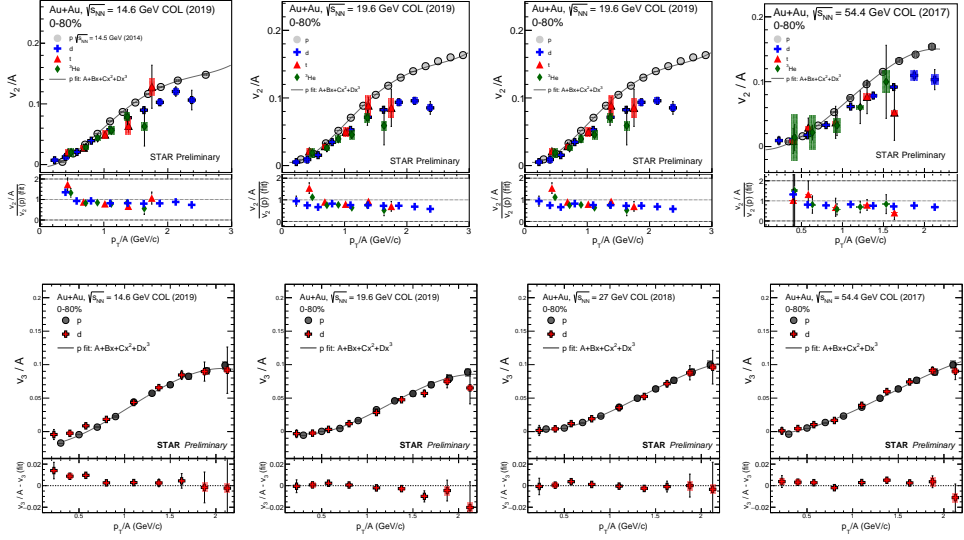


Figure 3. Mass number scaling of v_2 of p , d , t , and ${}^3\text{He}$ (top panel) and v_3 of p and d (bottom panel) as a function of p_T/A in minimum bias Au+Au collisions at $\sqrt{s_{NN}} = 14.6, 19.6, 27,$ and 54.4 GeV. Gray solid lines correspond to third order polynomial fits to v_2 and v_3 of p . The ratios of $[v_2/A]/\text{fit}$ for d , t , and ${}^3\text{He}$ and the differences of $[v_3/A]-\text{fit}$ for d are shown for each collision energy. Vertical lines and shaded bands at each marker represent statistical and systematic uncertainties, respectively.

3.3 Mass number scaling

Figure 3 shows the comparison of v_2/A and v_3/A of light nuclei as a function p_T/A , where A is the mass number of the corresponding nuclei, with v_2/A of proton ($A = 1$ for proton). The aim of this study is to compare v_2 and v_3 of light nuclei with the expectation of mass number scaling from the coalescence picture. According to the coalescence model, assuming v_2 (v_3) of proton and neutron is identical, for a light nuclei species N with mass number A , it is expected that, $v_{2(3)}^N(p_T) \approx A v_{2(3)}^p(p_T/A)$, where $v_{2(3)}^p$ is the elliptic (triangular) flow of proton [9–11]. It is observed that v_2 of d , t , and ${}^3\text{He}$ deviates from mass number scaling by 20-30% for the measured center-of-mass energies. However, v_3 of d is observed to follow mass number scaling within 10% for the measured center-of-mass energies.

3.4 Comparison with AMPT and coalescence calculations

To further test the hypothesis of light nuclei production from nucleon coalescence, string melting version of A Multi Phase Transport (AMPT, version ampt-v1.26t9b-v2.26t9b) model [12] in conjunction with a dynamic coalescence model is used to get a theoretical estimate of v_2 and v_3 of deuteron. In this model, the probability of coalescence is determined by the superposition of the Wigner function of the deuterons and nucleon phase-space distribution at freeze-out obtained from AMPT [13]. Figure 4 shows the comparison of v_2 and v_3 of d with the results from AMPT+Coalescence calculations. We have also compared v_2 and v_3 of p with AMPT model calculations. The data and model are observed to agree within uncertainties in the measured center-of-mass energies and p_T ranges. The agreement of v_2 and v_3 of d with the calculations from AMPT+Coalescence model indicate that final-state nucleon coalescence might be the dominant production mechanism of light nuclei.

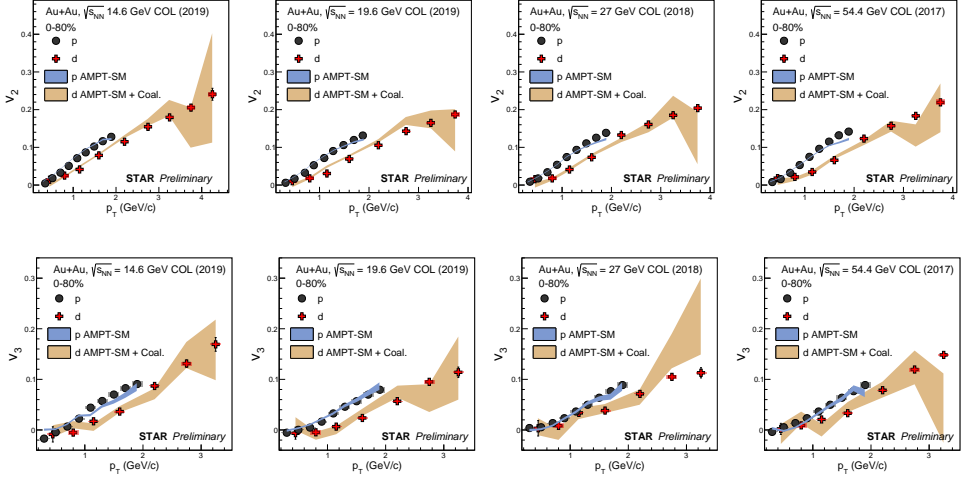


Figure 4. $v_2(p_T)$ (top panel) and $v_3(p_T)$ (bottom panel) of p and d compared with the results of AMPT+coalescence calculations (solid bands).

4 Summary

In summary, we have reported v_2 of d , t , and ^3He and v_3 of p and d in Au+Au collisions at $\sqrt{s_{NN}} = 14.6, 19.6, 27,$ and 54.4 GeV. A monotonic rise in light nuclei v_2 and v_3 with p_T in the measured energy and p_T range is observed. Mass ordering of v_2 and v_3 of light nuclei at low p_T is observed. v_2 of d is observed to show a strong centrality dependence being higher for peripheral collisions compared to central collisions. v_2 of light nuclei is found to deviate by 20-30% from mass number scaling in the measured center-of-mass energies whereas v_3 of d is observed to be in agreement with mass number scaling within 10%. In addition, we also observe that v_2 and v_3 of d are well described by the model calculations using AMPT+Coalescence, within uncertainties. These observations suggest that the final-state coalescence of nucleons might be the dominant mechanism of light nuclei production in heavy-ion collisions.

References

- [1] A. Andronic et al., Nature, **561**, 321–30 (2018).
- [2] S. T. Butler and C. A. Pearson, Phys. Rev. Lett., **129**, 836 (1963).
- [3] A. Schwarzschild and A. Zupancic, Phys. Rev. Lett., **129**, 854–862 (1963).
- [4] H. H. Gutbrod et al., Phys. Rev. Lett., **37**, 667 (1976).
- [5] H. Sato and K. Yazaki, Phys. Lett. B, **98**, 153–157 (1981).
- [6] Adamczyk L et al. (STAR Collaboration), Phys. Rev. C **94**, 034908 (2016).
- [7] Adam J et al. (STAR Collaboration) Phys. Rev. C **99**, 064905 (2019).
- [8] A. M. Poskanzer and S. A. Voloshin Phys. Rev. C **58**, 1671 (1998).
- [9] L. Adamczyk et al. (STAR Collaboration) Phys. Rev. C **94**, 034908 (2016).
- [10] T. Z. Yan, Y. G. Ma, X. Z. Cai et al., Phys. Lett. B, **638**, 50–54 (2006).
- [11] Y. Oh and C. M. Ko, Phys. Rev. C, **76**, 054910 (2007).
- [12] Zi-Wei Lin et al., Phys. Rev. C **72**, 064901 (2005).
- [13] L.-W. Chen et al., Nucl. Phys. A **729**, 809 (2003).